AIAA JOURNAL
Vol. 47, No. 3, March 2009

# Hierarchical Evaluation of Failure Parameters in Composite Plates

E. Carrera*
*Politecnico di Torino, 10129 Turin, Italy*
and
G. Giunta†
*Centre de Recherche Public Henri Tudor, L-1855 Luxembourg-Kirchberg*

DOI: 10.2514/1.38585

**This paper presents a failure analysis of simply supported, orthotropic plates subjected to global/local bending loadings via the Navier-type solution. Carrera's unified formulation is adopted in order to implement a large variety of two-dimensional theories. The minimum first-ply failure loading and the failure locations are obtained via classical, refined, zig-zag, layerwise, and mixed theories. The maximum stress, Tsai–Wu, Tsai–Hill, Hoffman, and Hashin failure criteria are assumed. The accuracy of two-dimensional theories is assessed via comparison with the three-dimensional Pagano's solution, which has here been extended to the considered cases. The influence of the side-to-thickness ratio, the aspect ratio, the material properties, the lamination layup, and the loading localization is investigated. A hierarchy among the Carrera's unified formulation two-dimensional models has been established.**



## Nomenclature

| | | |
|---|---|---|
| $a$ | = | plate dimension along the $x$ direction |
| $b$ | = | plate dimension along the $y$ direction |
| $E_L$ | = | Young's modulus in the direction parallel to the fibers |
| $E_T$ | = | Young's modulus in the direction perpendicular to the fibers |
| $f$ | = | component of the generic unknown vector |
| $F_j$, $F_\tau$ | = | thickness approximation functions |
| $f^k$ | = | component of the generic unknown vector at the $k$ layer |
| $g$ | = | part of the unknown dependending on $x$ and $y$ |
| $G_{\mathrm{LT}}$ | = | shear modulus in planes parallel to the fibers |
| $G_{\mathrm{TT}}$ | = | shear modulus in planes perpendicular to the fibers |
| $G^0_{\mathrm{LT}}$ | = | reference shear modulus |
| $g^k$ | = | part of the unknown dependending on $x$ and $y$ at $k$ layer |
| $h$ | = | total thickness of the plate |
| $h_k$ | = | thickness of the $k$ layer |
| $k$ | = | layer index |
| $k^*$ | = | localized loading application area parameter |
| $L_e$ | = | external work |
| $m$ | = | half-waves number along the $x$ direction |
| $\bar{m}$ | = | maximum half-waves number along the $x$ direction |
| $N$ | = | polynomial order |
| $n$ | = | half-waves number along the $y$ direction |
| $\bar{n}$ | = | maximum half waves number along the $y$ direction |
| $N_l$ | = | total number of layers |
| $P_j$ | = | Legendre's polynomial |
| $p_{zz}$ | = | localized bending loading |
| $p^0_{zz}$ | = | maximal amplitude of the localized bending loading |
| $R$ | = | shear strength on planes normal to the fibers |
| $S$ | = | shear strength on planes parallel to the fibers |
| $\mathbf{u}$ | = | displacement vector |
| $\mathbf{u}^k$ | = | $k$ layer displacement vector |
| $u_x$, $u_y$, $u_z$ | = | displacement components |
| $\tilde{u}_x$, $\tilde{u}_y$, $\tilde{u}_z$ | = | maximal amplitudes of the displacement components |
| $V$ | = | volume of the plate |
| $x$, $y$, $z$ | = | reference system coordinates |
| $X_c$, $X_t$ | = | compressive and tensile strength along the fibers |
| $Y_c$, $Y_t$ | = | compressive and tensile strength transverse to the fibers |
| $z_k$ | = | local through-the-thickness coordinate |
| $\delta$ | = | virtual variation operator |
| $\epsilon_p$, $\epsilon_n$ | = | in- and out-of-plane strain vectors |
| $\epsilon_{xx}$, $\epsilon_{xy}$, $\epsilon_{yy}$ | = | in-plane strain components |
| $\epsilon_{xz}$, $\epsilon_{yz}$, $\epsilon_{zz}$ | = | out-of-plane strain components |
| $\zeta_k$ | = | no-dimensional thickness coordinate |
| $\nu_{\mathrm{LT}}$ | = | Poisson's ratio in planes parallel to the fibers |
| $\nu_{\mathrm{TT}}$ | = | Poisson's ratio in planes perpendicular to the fibers |
| $\boldsymbol{\sigma}^k$ | = | $k$-layer stress vector |
| $\sigma_p$, $\sigma_n$ | = | in- and out-of-plane stress vectors |
| $\sigma_{xx}$, $\sigma_{xy}$, $\sigma_{yy}$ | = | in-plane stress components |
| $\sigma_{xz}$, $\sigma_{yz}$, $\sigma_{zz}$ | = | out-of-plane stress components |
| $\tilde{\sigma}_{xz}$, $\tilde{\sigma}_{yz}$, $\tilde{\sigma}_{zz}$ | = | maximal amplitudes of the out-of-plane stresses |
| $\Omega$ | = | reference midplane of the plate |

*Subscripts*

| | | |
|---|---|---|
| $G$ | = | unknown obtained via geometrical relations |
| $H$ | = | unknown obtained via Hooke's constitutive equations |
| $M$ | = | a priori modeled stress |

*Superscript*

| | | |
|---|---|---|
| $T$ | = | vector transpose operator |

Received 16 May 2008; revision received 24 September 2008; accepted for publication 26 November 2008. 

*Professor of Aerospace Structures and Aeroelasticity, Department of Aeronautic and Space Engineering, Corso Duca degli Abruzzi 24.

†Politecnico di Torino, Research Scientist, Department of Aeronautic and Space Engineering, Corso Duca degli Abruzzi 24, 10129 Turin, Italy; gaetano.giunta@polito.it.

## Introduction

OVER the last decades, composite materials have been applied more and more in the most advanced engineering fields, such as aeronautics, space, and automotive, due to the possibility of obtaining high values of stiffness-to-weight and strength-to-weight ratios. Accurate and effective prediction of failure parameters, such as minimum failure loadings and failure locations, is mandatory for their safe utilization and correct optimization. Highly accurate mechanical models are, therefore, required to effectively describe the mechanics of composites. To the best of the authors' knowledge, composite plate failure analysis was first treated by Turvey. Initial failure analysis of cross-ply laminated strips was addressed in [1], and rectangular plates undergoing bisinusoidal and uniform bending loadings were investigated in [2] and in [3], respectively. Square, angle-ply laminates were accounted for in [4]. Angle-ply plates, made of both glass and carbon fiber reinforced plastics, were considered in [5]. Classical theories based on the Cauchy [6], Poisson [7], and Kirchhoff [8] hypotheses were adopted in all of the previous works. Turvey [9] considers shear deformation effects by means of Reddy's higher-order shear deformation theory [10]. Initial failure loadings were obtained assuming the Tsai–Hill [11] failure criterion. The Navier-type closed-form solution was adopted. Kam and Jan [12] assumed a layerwise approach within the finite elements method. The displacement field was postulated to be linear along the thickness direction. Several failure criteria, such as the maximum stress/strain (see Reddy [13]), Tsai–Wu [14], Hoffman [15], and Tsai–Hill were adopted. The numerical results were confirmed by means of experimental data. Kam et al. [16] investigated thin laminated plates, accounting for nonlinear effects via the von Karman–Mindlin theory. Experimental investigations were carried out as well. The experimental results showed that the load-deflection relation may be nonlinear, even before the occurrence of first-ply failure. The results addressed in [16] were used by Karmakar and Sinha in order to validate the finite element proposed in [17] to study composite pretwisted rotating plates. A layerwise-based finite element was also formulated by Onkar et al. [18]. Stochastic first-ply failure loading was determined via the Tsai–Wu and Hoffman failure criteria. First-ply and post-first-ply failure was investigated by Reddy and Pandey [19,20] via the finite elements method. Failure loadings and locations were computed for several lamination configurations. Both bending and in-plane loadings were considered. In Reddy and Reddy [21], geometric nonlinearities were accounted for. The first-order shear deformation theory by Reissner [22] and Mindlin [23] was assumed. The macromechanical models of failure, such as the maximum stress/strain, Tsai–Wu, Hoffman, and Tsai–Hill criteria, were assumed. As far as failure models are concerned, several failure criteria for composite structures have been formulated over the past few decades. Classical phenomenological criteria have been presented in Sih and Skudra [24], Soni [25], and Soden et al. [26]. The drawbacks and benefits of some of them were investigated at the World Wide Failure Exercise organized and documented by Hinton and Soden [27], in which Puck's criterion [28–30] resulted to be one of the most effective. NASA has developed its own criterion named LaRC04 [31]. The works by Basu et al. [32–34] are worth mentioning. Progressive damage models of compressive fiber failure and kink banding in particular have been presented. Multi-axial loading conditions have been accounted for. The proposed models have been implemented in ABAQUS and have been validated against experimental data. The compressive strength of a lamina has been found to be strongly dependent on the nonlinear shear response, the material local point, the local stress state, and local fiber rotation. The concept of a fixed compressive strength has been shown to be not appropriate. Nonlinear constitutive models, at least in the transverse direction, should be adopted. The presents work concerns a failure analysis of composite plates via a systematic approach to two-dimensional modeling named Carrera's unified formulation (CUF), as named by Demasi [35]. The modeling is based on the identification of three main features that two-dimensional models can be formulated on: 1) a priori, primary variables, 2) an equivalent single layer (ESL) or layerwise (LW) approach, and 3) the order of the through-the-thickness polynomial approximation. A common formal notation allows one to formulate a large variety of two-dimensional theories, according to the previous three common points. CUF accounts for higher-order theories based on the principle of virtual displacement (PVD) or on Reissner's mixed variational theorem (RMVT) (see Reissner [36]). Transverse normal and shear deformations are also accounted for. Models that fulfill the $C_z^0$ requirement (see Carrera [37]) intrinsically at laminae interface or via Murakami's zig-zag function (see Murakami [38] and Carrera [39,40]) are accounted for. Classical theories, based on the Kirchhoff [8] and Reissner kinematics, are obtained as particular cases. An exhaustive exposition of the theoretical background, together with a detailed numerical investigation of the static and dynamic response of composite plates and shells, can be found in Carrera [41]. CUF has been adopted by Carrera and Giunta [42,43] in order to investigate displacements, stresses, and failure loadings in the case of isotropic plates undergoing distributed and localized bending loadings. Carrera and Ciuffreda [44,45] and Carrera and Demasi [46] have accounted for CUF models in order to investigate the mechanics of composites and sandwich plates subjected to localized loadings via the Navier closed-form solution and FEM, respectively. The Navier-type closed-form solution is assumed in this work. The minimum failure-loading value and location are investigated. The maximum stress, Tsai–Wu, Tsai–Hill, Hoffman, and Hashin [47] failure criteria have been adopted. Geometrical and material nonlinearities have been discarded. Further work will be devoted to their investigation and implementation. The influence of the side-to-thickness ratio, the aspect ratio, and the material properties have been investigated. Plates are considered to undergo distributed and localized uniform loadings. The accuracy of the two-dimensional models has been assessed via a comparison with the three-dimensional solution obtained by Pagano [48]. Apart from its engineering meaning and importance, the minimum failure loading and its location can be regarded as parameters that allow one to globally establish the accuracy of the proposed two-dimensional model. In this respect, the maximum stress failure criterion assumes a relevant role, because, due to its formulation, it avoids possible error compensations that may yield apparently accurate results. CUF two-dimensional theories have been hierarchically classified according to their accuracy.

## Hierarchical Plate Models

The plate geometry, the reference system, and the displacement components are shown in Fig. 1. A large variety of two-dimensional theories can be formulated on the basis of different kinematic assumptions. The two-dimensional theories adopted in this work are all formulated via CUF. The main principles, on which CUF is based, are presented here in a concise manner. The detailed treatment can be found in Carrera [41]. Some common points characterize the formulation of the two-dimensional mechanical models of plates. Three of them are identified in CUF: the type of the primary unknowns, the through-the-thickness approximation order, and the manner that such an approximation is imposed.

### Choice of the Unknown Variables and Related Variational Statements

The choice of the variational statement in order to derive the governing differential equations determines the main unknowns.

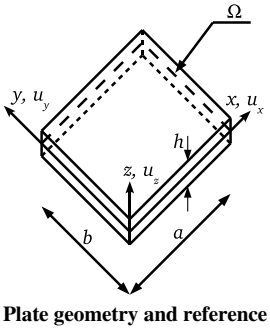


**Fig. 1 Plate geometry and reference system.**

Within CUF, either the PVD or the RMVT can be adopted. In the case of the PVD, models based on displacement components are formulated

$$\int_V \left(\delta\boldsymbol{\epsilon}_{pG}^T \boldsymbol{\sigma}_{pH} + \delta\boldsymbol{\epsilon}_{nG}^T \boldsymbol{\sigma}_{nH}\right) \mathrm{d}V = \delta L_e \tag{1}$$

in which

$$\boldsymbol{\epsilon}_p = \begin{Bmatrix} \epsilon_{xx} \\ \epsilon_{yy} \\ \epsilon_{xy} \end{Bmatrix}, \quad \boldsymbol{\sigma}_p = \begin{Bmatrix} \sigma_{xx} \\ \sigma_{yy} \\ \sigma_{xy} \end{Bmatrix}, \quad \boldsymbol{\epsilon}_n = \begin{Bmatrix} \epsilon_{xz} \\ \epsilon_{yz} \\ \epsilon_{zz} \end{Bmatrix}, \quad \boldsymbol{\sigma}_n = \begin{Bmatrix} \sigma_{xz} \\ \sigma_{yz} \\ \sigma_{zz} \end{Bmatrix} \tag{2}$$

Subscript $G$ means that the strain components have been obtained by means of derivation of the displacement field and $H$ stands for unknown components computed via the Hooke's generalized law. The models based on the RMVT

$$\int_V \left[\delta\boldsymbol{\epsilon}_{pG}^T \boldsymbol{\sigma}_{pH} + \delta\boldsymbol{\epsilon}_{nG}^T \boldsymbol{\sigma}_{nM} + \delta\boldsymbol{\sigma}_{nM}^T (\boldsymbol{\epsilon}_{nG} - \boldsymbol{\epsilon}_{nH})\right] \mathrm{d}V = \delta L_e \tag{3}$$

are characterized by both displacement and out-of-plane stress components. Subscript $M$ signifies that the out-of-plane stress components are assumed to be primary unknowns in the model. The continuity of $\boldsymbol{\sigma}_n$, which is due to the laminae interface equilibrium, is ensured by this assumption.

### Approximation Order

The generic component $f(x, y, z)$ of the main unknown vector can be expressed in the following manner:

$$f(x, y, z) = F_j(z) g_j(x, y) \quad j = 0, 1, \ldots, N \tag{4}$$

The term $F_j(z)$ is an axiomatically postulated function of $z$. It is characteristic of the two-dimensional modeling. Different functions were used to approximate the through-the-thickness variation. Touratier [49] proposed sine functions, whereas hyperbolic sinus and cosines functions were adopted by Soldatos [50]. Within CUF, $F_j(z)$ is a polynomial function whose maximum order is $N$. This is considered to be four. The type of the polynomials depends on the approach to the approximation. Function $g_j(x, y)$ represents the variation of the unknown versus the in-plane coordinates. According to the Navier solution, this is a combination of sinus and cosines functions depending on the unknown component. The following relations hold by considering Fourier's series expansion of a general bending loading and due to the problem linearity:

$$\begin{aligned}
(u_x, \sigma_{xz}) &= (\tilde{u}_x(z), \tilde{\sigma}_{xz}(z)) \cos\left(\frac{m\pi}{a}x\right) \sin\left(\frac{n\pi}{b}y\right) \\
(u_y, \sigma_{yz}) &= (\tilde{u}_y(z), \tilde{\sigma}_{yz}(z)) \sin\left(\frac{m\pi}{a}x\right) \cos\left(\frac{n\pi}{b}y\right) \quad \begin{matrix} m = 1, 2, \ldots, \bar{m} \\ n = 1, 2, \ldots, \bar{n} \end{matrix} \\
(u_z, \sigma_{zz}) &= (\tilde{u}_z(z), \tilde{\sigma}_{zz}(z)) \sin\left(\frac{m\pi}{a}x\right) \sin\left(\frac{n\pi}{b}y\right)
\end{aligned} \tag{5}$$

### Approach to the Through-the-Thickness Approximation

Each unknown is defined continuously along the thickness of the laminate in the equivalent single layer (ESL) models, see Fig. 2. Average mechanical properties are considered in order to consider the transversal anisotropy. For ESL models, the polynomial terms $\{F_j(z), j = 0, \ldots, N\}$ in Eq. (4) are the elements of the classical polynomial base

$$F_j(z) = z^j \quad j = 0, 1, \ldots, N \tag{6}$$

According to Eq. (6), CUF yields theories that account for both normal and transverse shear deformation. The kinematic field of the classical theories, such as the first-order shear deformation theory (FSDT), can be obtained posing $N = 1$ for $u_x$ and $u_y$ and $N = 0$ for $u_z$ in Eq. (6). The displacement and the out-of-plane stress components must be $C^0$ class with respect to the through-the-thickness coordinate, due to the transversal anisotropy. ESL theories are based on $C^\infty$ class functions instead. The zig-zag effect can be retrieved, within the ESL approach, through Murakami's zig-zag function $F_{N+1}(z) = (-1)^k \zeta_k$. Equation (7) presents the approximating polynomial base in the case of ESL models with Murakami's function

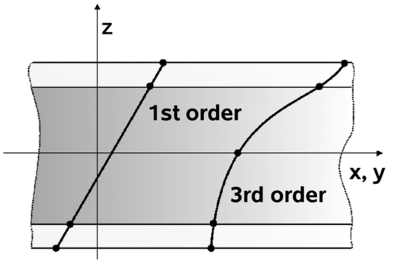


**Fig. 2 Generic main unknown $f$ approximation via ESL first- and third-order theories.**

$$F_j(z) = \begin{cases} z^j & j = 0, 1, \ldots, N \\ (-1)^k \zeta_k & j = N + 1 \end{cases} \tag{7}$$

$\zeta_k$ is the $k$-layer local, dimensionless coordinate along the thickness such that $-1 \leq \zeta_k \leq 1$. The third-order ESL zig-zag theory is shown in Fig. 3. The ESL approach is no longer suitable in the case of significant unknown gradients due to the presence of local phenomena such as localized loadings or pronounced material discontinuity in the thickness direction. ESL approximation is intrinsically unable to fulfill the $C_z^0$ requirements because the primary unknowns are approximated via continuous functions with continuous derivatives. The derived unknowns are also not continuous due to the material properties discontinuity along the thickness. An LW description, that is, layer by layer, should be considered instead. According to the LW approach, Eq. (4) holds for each layer:

$$\begin{aligned}
f^k(x, y, \zeta_k(z)) = F_j(\zeta_k(z)) g_j^k(x, y) \qquad & j = 0, 1, \ldots, N \\
& k = 1, \ldots, N_l
\end{aligned} \tag{8}$$

$N_l$ is the total number of layers. The integrity of the plate is insured by imposing the interlaminar continuity: the displacement and the out-of-plane stress components must be continuous at layer interfaces. $F_j(\zeta_k)$ is a linear combination of Legendre's polynomial functions:

$$\begin{aligned}
F_0(\zeta_k) = \frac{P_0(\zeta_k) - P_1(\zeta_k)}{2}, \qquad F_1(\zeta_k) = \frac{P_0(\zeta_k) + P_1(\zeta_k)}{2} \\
F_r(\zeta_k) = [P_r(\zeta_k) - P_{r-2}(\zeta_k)] \qquad r = 2, 3, \ldots, N
\end{aligned} \tag{9}$$

in which $\{P_j(\zeta_k)\colon j = 0, 1, \ldots, N\}$ are defined through the following recursive formula:

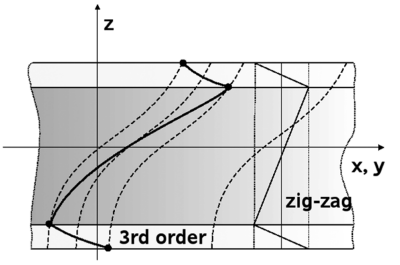


**Fig. 3 Generic main unknown $f$ approximation via ESL third-order model with Murakami's zig-zag function.**

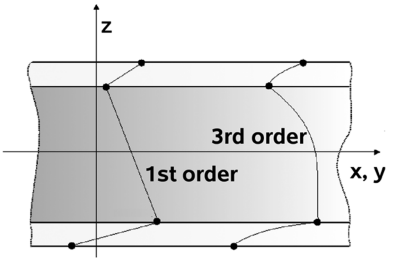


**Fig. 4 Generic main unknown $f$ approximation via LW first- and third-order theories.**

$$P_0(\zeta_k) = 1$$
$$P_1(\zeta_k) = \zeta_k(n+1)P_{n+1}(\zeta_k) = (2n+1)\zeta_k P_n(\zeta_k) - nP_{n-1}(\zeta_k)$$
$$n = 1, 2, \ldots, N-1 \tag{10}$$

Legendre's polynomials have been chosen in order to easily impose the displacement congruency and the out-of-plane stresses equilibrium between two consecutive layers. Figure 4 shows the first- and third-order LW approximations of $f$.

#### Acronym System and Unified Notation

The definition of a manner to address the two-dimensional models that can be derived through CUF is needed. Figure 5 shows the adopted acronym system. The first letter, either L or E, specifies whether an LW or an ESL approach is assumed. The second letter indicates the variational statement: D for PVD or M in the case of RMVT. The number at the end of the acronym represents the polynomial approximation order. The third letter is optional. It may be a Z to indicate that Murakami's zig-zag function is adopted or a D for theories that discard the transverse deformation, that is, transverse displacement is constant with respect to $z$. Some examples of CUF theories follow. The generic EDN model is an ESL, displacement-based theory in which an $N$-order polynomial approximation is adopted:

$$\begin{aligned} u_x(x,y,z) &= u_{x0} + u_{x1}z + u_{x2}z^2 + \cdots + u_{xN}z^N \\ u_y(x,y,z) &= u_{y0} + u_{y1}z + u_{y2}z^2 + \cdots + u_{yN}z^N \\ u_z(x,y,z) &= u_{z0} + u_{z1}z + u_{z2}z^2 + \cdots + u_{zN}z^N \end{aligned} \tag{11}$$

In the vectorial notation

$$\mathbf{u} = F_0\mathbf{u}_0 + F_1\mathbf{u}_1 + \cdots + F_N\mathbf{u}_N = F_\tau\mathbf{u}_\tau \qquad \tau = 0, 1, \ldots, N \tag{12}$$

The kinematic field of the generic EDZN theory is

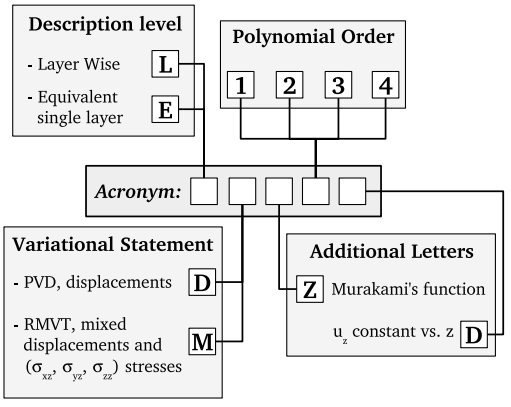


**Fig. 5 CUF acronym system.**

$$\begin{aligned} u_x(x,y,z) &= u_{x0} + u_{x1}z + u_{x2}z^2 + \cdots + u_{xN}z^N + (-1)^k\zeta_k u_{xN+1} \\ u_y(x,y,z) &= u_{y0} + u_{y1}z + u_{y2}z^2 + \cdots + u_{yN}z^N + (-1)^k\zeta_k u_{yN+1} \\ u_z(x,y,z) &= u_{z0} + u_{z1}z + u_{z2}z^2 + \cdots + u_{zN}z^N + (-1)^k\zeta_k u_{zN+1} \end{aligned} \tag{13}$$

In the compact notation

$$\mathbf{u} = F_0\mathbf{u}_0 + F_1\mathbf{u}_1 + \cdots + F_N\mathbf{u}_N + F_{N+1}\mathbf{u}_{N+1} = F_\tau\mathbf{u}_\tau \qquad \tau = 0, 1, \ldots, N, N+1 \tag{14}$$

in which $\{F_i = z^i\colon i = 0, 1, \ldots, N\}$ and $F_{N+1}$ is Murakami's function. In the LMN theory, an $N$-order polynomial approximation is assumed layer by layer for both displacement and out-of-plane stress components. The unified vectorial notation is

$$\begin{aligned} \mathbf{u}^k &= F_0\mathbf{u}_0^k + F_1\mathbf{u}_1^k + \cdots + F_N\mathbf{u}_N^k = F_\tau\mathbf{u}_\tau^k \\ \boldsymbol{\sigma}^k &= F_0\boldsymbol{\sigma}_0^k + F_1\boldsymbol{\sigma}_1^k + \cdots + F_N\boldsymbol{\sigma}_N^k = F_\tau\boldsymbol{\sigma}_\tau^k \end{aligned} \quad \tau = 0, 1, \ldots, N \qquad k = 1, 2, \ldots, N_l \tag{15}$$

The $F_\tau$ terms are presented in Eq. (9). The considered theories can be unified considering that FSDT is a peculiar case of ESL model. ESL theories can be regarded as particular cases of LW models in which the number of layers is equal to the unit and the elements of classical polynomial base are assumed as approximating functions. This unifying idea leads to the assumption of the common notation in Eqs. (12), (14), and (15). This facilitates the derivation of the governing equations. For the sake of brevity, the governing equations are not reported. For more details refer to Carrera [41].

## Results and Discussion

First-ply minimum failure loadings and failure locations are computed for cross-ply simply supported plates. The phenomenological maximum stress, Tsai–Wu, Tsai–Hill, Hoffman, and Hashin criteria are adopted. For the sake of brevity and because they are well known, they are not reported here. The first-ply failure loading can be obtained for each criterion via some algebraic manipulations and thanks to the problem linearity. The symmetric configuration $[0/90]_S$ is studied above all, even though the influence of the lamination sequence on the minimum failure loading is investigated. Ply angles are measured with respect to the $x$ axis. The plies are all made of T300/5208 graphite/epoxy. The mechanical material properties are $E_L = 132.5 \times 10^3$ MPa, $E_T = 10.8 \times 10^3$ MPa, $G_{LT} = 5.7 \times 10^3$ MPa, $G_{TT} = 3.4 \times 10^3$ MPa, $\nu_{LT} = 0.24$, and $\nu_{TT} = 0.49$. The material strengths are $X_t = 1515$ MPa, $X_c = 1697$ MPa, $Y_t = 43.8$ MPa, $Y_c = 43.8$ MPa, $S = 86.9$ MPa, and $R = 67.6$ MPa. The plies all have the same thickness. Unless otherwise specified, the plate sides are of equal length. A uniform loading acts on the plate top, and it is directed along the positive direction of the through-the-thickness axis. The $\bar{m}$ and $\bar{n}$ in Eq. (5) are assumed to be equal to 31. The side-to-thickness parameter $(a/h)$ is considered to be as high as 100 and as low as 2; thin and very thick plates are dealt with. The analyses were carried out in order to investigate the effects on the failure loadings and the accuracy of the CUF two-dimensional models of the side-to-thickness ratio $(a/h)$, the aspect ratio $(b/a)$, the material properties ($E_L/E_T$ and $G_{LT}$), the laminate layup, and the loading application area. Pagano's three-dimensional exact solution is also adopted in order to assess and hierarchically classify the CUF models. Out-of-plane stresses, in the case of FSDT, are computed via integration of the indefinite equilibrium equations, see Carrera [51].

#### Influence of the Side-to-Thickness Ratio

The minimum first-ply failure loadings and locations computed via the three-dimensional exact solution and CUF two-dimensional models are presented in Tables 1–5 for several values of the side-to-thickness ratio. In the case where a two-dimensional theory predicts a failure location that is coincident with the location obtained via the exact three-dimensional solution, the ratio between the two solutions is reported. The considered criteria all predict the failure to occur at

**Table 1 Minimum first-ply failure-loading values, locations, and errors via the maximum stress criterion**

| $a/h$ | 100 | 50 | 10 | 5 | 2 |
|---|---|---|---|---|---|
| MPa | $\times 10^{-2}$ | $\times 10^{-1}$ | $\times 1$ | $\times 10$ | $\times 10$ |
| 3-D | 6.6512[a] | 2.6423[a] | 5.4948[a] | 1.5328[a] | 3.9192[a] |
| FSDT | 6.6590, 1.00[b] | 2.6547, 1.00 | 6.0525, 1.10 | 2.0107, 1.31 | 4.5594, 1.16 |
| ED4D | 6.6555, 1.00 | 2.6491, 1.00 | 5.7917, 1.05 | 1.7801, 1.16 | 4.5454, 1.16 |
| ED4 | 6.6380, 1.00 | 2.6374, 1.00 | 5.4977, 1.00 | 1.5365, 1.00 | 3.8968, 0.99 |
| EDZ3 | 6.6550, 1.00 | 2.6427, 1.00 | 5.4227, 0.99 | 1.4721, 0.96 | 3.4643, 0.88 |
| LD2 | 6.6509, 1.00 | 2.6419, 1.00 | 5.4759, 1.00 | 1.5139, 0.99 | 3.7740, 0.96 |
| LD4 | 6.6512, 1.00 | 2.6423, 1.00 | 5.4953, 1.00 | 1.5333, 1.00 | 3.8918, 0.99 |
| LM2 | 6.6512, 1.00 | 2.6423, 1.00 | 5.4931, 1.00 | 1.5269, 1.00 | 3.8404, 0.98 |
| LM4 | 6.6512, 1.00 | 2.6423, 1.00 | 5.4950, 1.00 | 1.5329, 1.00 | 3.8931, 0.99 |

[a]Failure location at the top of the center point.
[b]2-D–3-D minimum failure-loading ratio in the case of coincident failure locations.

**Table 2 Minimum first-ply failure-loading values, locations, and errors via the Tsai–Wu criterion**

| $a/h$ | 100 | 50 | 10 | 5 | 2 |
|---|---|---|---|---|---|
| MPa | $\times 10^{-2}$ | $\times 10^{-1}$ | $\times 1$ | $\times 10$ | $\times 10$ |
| 3-D | 7.3544[a] | 2.9307[a] | 6.5436[b] | 1.9672[b] | 4.5953[b] |
| FSDT | 7.3635, 1.00[c] | 2.9453, 1.00 | 6.8624, 1.05 | 2.2243, 1.13 | 5.3600, - |
| ED4D | 7.3595, 1.00 | 2.9388, 1.00 | 6.5566, 1.00 | 1.9689, 1.00 | 5.4731, - |
| ED4 | 7.3391, 1.00 | 2.9250, 1.00 | 6.5541, 1.00 | 1.9889, 1.01 | 4.5673, - |
| EDZ3 | 7.3589, 1.00 | 2.9312, 1.00 | 6.4576, 0.99 | 1.8880, - | 4.2031, 0.91 |
| LD2 | 7.3541, 1.00 | 2.9303, 1.00 | 6.5192, 1.00 | 1.9468, 0.99 | 4.4862, 0.98 |
| LD4 | 7.3544, 1.00 | 2.9308, 1.00 | 6.5436, 1.00 | 1.9673, 1.00 | 4.5770, 1.00 |
| LM2 | 7.3544, 1.00 | 2.9307, 1.00 | 6.5425, 1.00 | 1.9669, 1.00 | 4.5345, 0.99 |
| LM4 | 7.3544, 1.00 | 2.9308, 1.00 | 6.5433, 1.00 | 1.9669, 1.00 | 4.5783, 1.00 |

[a]Failure location at the top of the center point.
[b]Failure location at the bottom of the center point.
[c]2-D–3-D minimum failure-loading ratio in the case of coincident failure locations.

**Table 3 Minimum first-ply failure-loading values, locations, and errors via the Tsai–Hill criterion**

| $a/h$ | 100 | 50 | 10 | 5 | 2 |
|---|---|---|---|---|---|
| MPa | $\times 10^{-2}$ | $\times 10^{-1}$ | $\times 1$ | $\times 10$ | $\times 10$ |
| 3-D | 6.3680[a] | 2.5417[a] | 5.6318[b] | 1.7533[b] | 6.5574[b] |
| FSDT | 6.3750, 1.00[c] | 2.5528, 1.00 | 5.8875, 1.05 | 1.9794, 1.13 | 6.6875, - |
| ED4D | 6.3717, 1.00 | 2.5476, 1.00 | 5.6388, 1.00 | 1.7525, 1.00 | 5.4468, - |
| ED4 | 6.3564, 1.00 | 2.5373, 1.00 | 5.6392, 1.00 | 1.7704, 1.01 | 5.5116, - |
| EDZ3 | 6.3714, 1.00 | 2.5420, 1.00 | 5.5675, 0.99 | 1.6892, 0.96 | 5.4800, - |
| LD2 | 6.3678, 1.00 | 2.5413, 1.00 | 5.6136, 1.00 | 1.7368, 0.99 | 6.3149, - |
| LD4 | 6.3680, 1.00 | 2.5417, 1.00 | 5.6319, 1.00 | 1.7533, 1.00 | 6.5569, 1.00 |
| LM2 | 6.3680, 1.00 | 2.5417, 1.00 | 5.6310, 1.00 | 1.7530, 1.00 | 6.4304, - |
| LM4 | 6.3680, 1.00 | 2.5417, 1.00 | 5.6317, 1.00 | 1.7530, 1.00 | 6.5550, 1.00 |

[a]Failure location at the top of the center point;
[b]Failure location at the bottom of the center point.
[c]2-D–3-D minimum failure-loading ratio in the case of coincident failure locations.

**Table 4 Minimum first-ply failure-loading values, locations, and errors via the Hoffman criterion**

| $a/h$ | 100 | 50 | 10 | 5 | 2 |
|---|---|---|---|---|---|
| MPa | $\times 10^{-2}$ | $\times 10^{-1}$ | $\times 1$ | $\times 10$ | $\times 10$ |
| 3-D | 6.2925[a] | 2.5116[a] | 5.6958[b] | 1.7698[b] | 6.6041[b] |
| FSDT | 6.2993, 1.00[c] | 2.5225, 1.00 | 5.9552, 1.05 | 1.9982, 1.13 | 6.6613, - |
| ED4D | 6.2961, 1.00 | 2.5174, 1.00 | 5.7030, 1.00 | 1.7692, 1.00 | 5.4265, - |
| ED4 | 6.2811, 1.00 | 2.5073, 1.00 | 5.7033, 1.00 | 1.7872, 1.01 | 5.5116, - |
| EDZ3 | 6.2958, 1.00 | 2.5119, 1.00 | 5.6303, 0.99 | 1.7047, 0.96 | 5.4800, - |
| LD2 | 6.2923, 1.00 | 2.5112, 1.00 | 5.6771, 1.00 | 1.7531, 0.99 | 6.3149, - |
| LD4 | 6.2925, 1.00 | 2.5116, 1.00 | 5.6958, 1.00 | 1.7698, 1.00 | 6.6035, 1.00 |
| LM2 | 6.2925, 1.00 | 2.5116, 1.00 | 5.6949, 1.00 | 1.7695, 1.00 | 6.4304, - |
| LM4 | 6.2925, 1.00 | 2.5116, 1.00 | 5.6956, 1.00 | 1.7696, 1.00 | 6.6017, 1.00 |

[a]Failure location at the top of the center point.
[b]Failure location at the bottom of the center point.
[c]2-D–3-D minimum failure-loading ratio in the case of coincident failure locations.

**Table 5 Minimum first-ply failure-loading values, locations, and errors via the Hashin criterion**

| $a/h$ | 100 | 50 | 10 | 5 | 2 |
|---|---|---|---|---|---|
| MPa | $\times 10^{-2}$ | $\times 10^{-1}$ | $\times 1$ | $\times 10$ | $\times 10$ |
| 3-D | 6.6435[a] | 2.6303[a] | 5.0057[a] | 1.1954[a] | 2.2270[a] |
| FSDT | 6.6513, 1.00[b] | 2.6426, 1.00 | 5.4632, 1.09 | 1.4621, 1.22 | 3.1583, 1.42 |
| ED4D | 6.6478, 1.00 | 2.6370, 1.00 | 5.2503, 1.05 | 1.3383, 1.12 | 2.7399, 1.23 |
| ED4 | 6.6303, 1.00 | 2.6254, 1.00 | 5.0081, 1.00 | 1.1976, 1.00 | 2.2200, 1.00 |
| EDZ3 | 6.6474, 1.00 | 2.6307, 1.00 | 4.9459, 0.99 | 1.1586, 0.97 | 2.0785, 0.93 |
| LD2 | 6.6432, 1.00 | 2.6298, 1.00 | 4.9901, 1.00 | 1.1840, 0.99 | 2.1814, 0.98 |
| LD4 | 6.6435, 1.00 | 2.6303, 1.00 | 5.0061, 1.00 | 1.1957, 1.00 | 2.2185, 1.00 |
| LM2 | 6.6435, 1.00 | 2.6302, 1.00 | 5.0037, 1.00 | 1.1914, 1.00 | 2.1990, 0.99 |
| LM4 | 6.6435, 1.00 | 2.6303, 1.00 | 5.0060, 1.00 | 1.1954, 1.00 | 2.2190, 1.00 |

[a]Failure location at the top of the center point.
[b]2-D–3-D minimum failure-loading ratio in the case of coincident failure locations.

the top of the center point in the case of $a/h$ as low as 50. For $a/h$ as high as 10, the polynomial criteria yield a failure that occurs at the bottom of the plate, whereas for the maximum stress and Hashin failure criteria, the top of the center point fails first. This is due to the importance that the normal out-of-plane stress component $\sigma_{zz}$ assumes on each criterion. In all of the cases, failure is due to the normal stress components. The Tsai–Wu criterion is the least conservative for $a/h \geq 5$, whereas for very thick plates, the Hoffman criterion yields the highest minimum failure load. This last criterion is the most conservative for $a/h \geq 50$. In all of the remaining cases, the minimum among the minimum failure loads is predicted by the Hashin criterion. According to this criterion, failure is due to the tension of the matrix. Failure is predicted to occur at the plate top, which is in tension, and in the case of fiber failure the Hashin criterion would yield the same failure value as the maximum stress criterion. The values are quite widespread; the ratio between the minimum and the maximum values is equal to 0.86 for $a/h = 100$ and 50, and it decreases to 0.34 in the case of very thick plates. As far as two-dimensional models are concerned, FSDT matches the exact solution for $a/h$ as low as 50. For $a/h = 10$, the results differ from the exact solution by about 10% in the case of the maximum stress and Hashin criteria and about 5% for the others. FSDT yields overestimated results, that is, it is not conservative. FSDT seems to predict better results than higher-order ESL models in the case of very thick plates, but the failure location is different from the three-dimensional solution. ED4D yields accurate results for $a/h \geq 5$ in the case of Tsai's and Hoffman's criteria. It yields less accurate results for the maximum stress and Hashin criteria than FSDT does. ED4 slightly underestimates the failure loads for $a/h \geq 50$, and, in the case of very thick plates, it overestimates them by about 1% for $a/h = 10$ and 5. EDZ3 behaves in the opposite manner. LW models are very accurate for any value of the side-to-thickness ratio. In most cases, they are conservative. In the cases in which they are not conservative, the difference from the exact solution is negligible.

### Influence of the Aspect Ratio

Figures 6 and 7 present the effect of the aspect ratio on the minimum failure loading of thin and thick plates, respectively, via the maximum stress and Tsai–Wu failure criteria. The change in slope is due to a change in the failure location. As $a/h$ is constant and $b/a$ increases, the considered criteria all yield matching

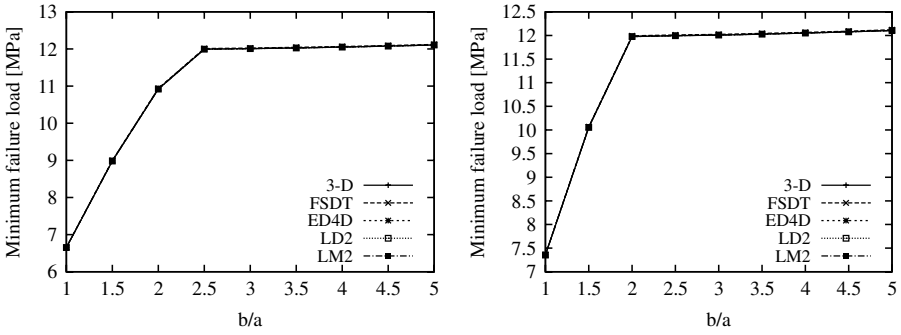


**Fig. 6 Minimum failure loading vs the aspect ratio via the a) maximum stress and b) Tsai–Wu criteria for thin plates.**

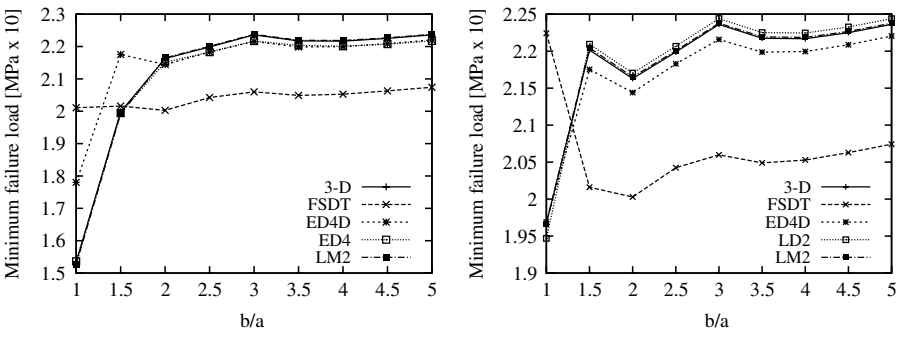


**Fig. 7 Minimum failure loading vs the aspect ratio via the a) maximum stress and b) Tsai–Wu criteria for thick plates.**

failure-loading values and locations. This is due to the fact that the higher the aspect ratio, the less important the thickness influence. The plate starts to resemble a beam whose mechanics is governed by bending; for $b/a$ equal to 5 and $a/h \geq 10$, failure is experienced at the bottom of the corner points. It is due to the $\sigma_{xy}$ stress component. The failure-loading value reaches a horizontal asymptote in correspondence with a threshold value of the aspect ratio, which depends on the criterion and on the value of the side-to-thickness ratio. In the case of the Tsai–Wu criterion and $a/h = 5$, negative slopes are present, that is, increasing the aspect ratio might not positively affect the failure mechanics. The same behavior has been found in the case of the Tsai–Hill and Hoffman criteria. For $a/h \geq 10$, FSDT and ED4D converge to the exact solution for $b/a < 5$ for each criterion. In the case of thick plates, higher values of the aspect ratio should be considered in order to reduce the thickness influence and, thus, to obtain convergence. Second-order LW models match the three-dimensional exact solution for any value of the aspect ratio and of the side-to-thickness ratio.

#### Influence of the Material Properties

Figure 8 shows the influence of the $E_L/E_T$ ratio on the first-ply minimum failure loading in the case of $a/h$ equal to 10. The addressed failure criteria are all adopted. $E_L/E_T$ is considered to be as low as 5 and as high as 55. For the results presented in Tables 1–5 to $E_L/E_T$ is equal to about 12. As far as the three-dimensional exact solution is concerned, increasing $E_L/E_T$ makes the fiber a preferred loading path and $\sigma_{yy}$ decreases in the 0 deg plies. The minimum failure loading, therefore, increases. The changes in slope are due to the failure location, which shifts from the center point to the points $\{(x, y)\colon x = 0, a; y = b/2\}$. The slope of the failure load decreases in correspondence to these points. The failure is governed by the out-of-plane shear stress $\sigma_{xz}$, which is not very influenced by $E_L/E_T$ as $\sigma_{xx}$ or $\sigma_{yy}$. No failure location shifting is encountered in the case of the Tsai–Hill or Hashin criteria. Higher-order ESL models, accounting for both transverse shear and normal deformation, yield accurate results. Transverse normal deformation plays an important role, as shown by the comparison between the ED4 and ED4D models. In the case of maximum stress criterion, ED4D anticipates the failure location shifting. Its accuracy increases for $E_L/E_T \geq 40$, because failure is due to the out-of-plane shear stress $\sigma_{xz}$. LW models yield accurate results. In the case of mixed models, a quadratic approximation is sufficient to match the three-dimensional exact solution. The dependency of the first-ply minimum failure loading on the shear modulus $G_{LT}$ is presented in Figs. 9 and 10 and for the case of $a/h = 10$ and 5, respectively. The maximum stress and Hoffman criteria are adopted. The values of the shear modulus are normalized with respect to the reference value $G^0_{LT} = 5.7 \times 10^3$ MPa. A critical value, after which the minimum failure load decreases, can be identified. The critical values depend on the failure criterion and on the side-to-thickness parameter. For higher values of $G_{LT}/G^0_{LT}$ than the critical value, the failure location shifts from the plate center to the top of the corner points. A loading redistribution from the normal stress components to the in-plane shear component $\sigma_{xy}$ occurs due to the growth of the shear stiffness. After the critical value, the material cannot withstand the growth of $\sigma_{xy}$. FSDT yields overestimated results. Results via ED4D for $a/h = 10$ are more accurate, because the normal out-of-plane stress is no longer involved in the failure. For

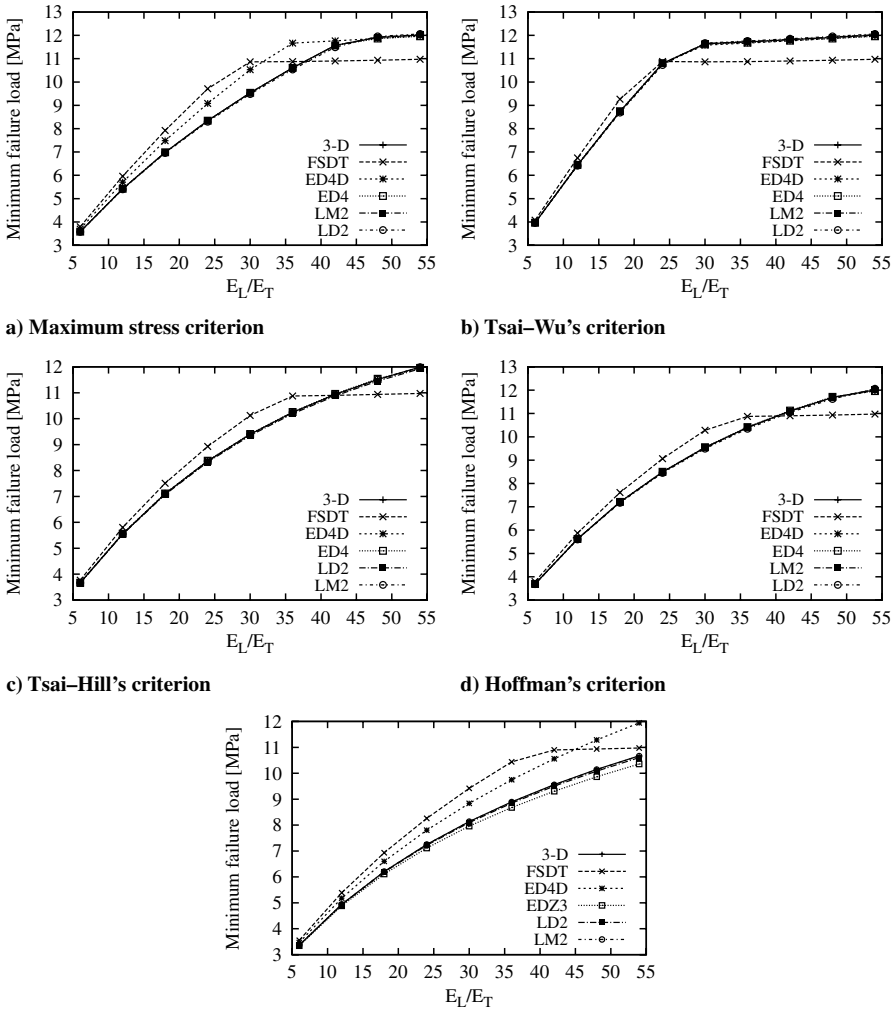


a) Maximum stress criterion

b) Tsai–Wu's criterion

c) Tsai–Hill's criterion

d) Hoffman's criterion

e) Hashin's criterion

**Fig. 8 Minimum failure loads vs $E_L/E_T$ for $a/h = 10$.**

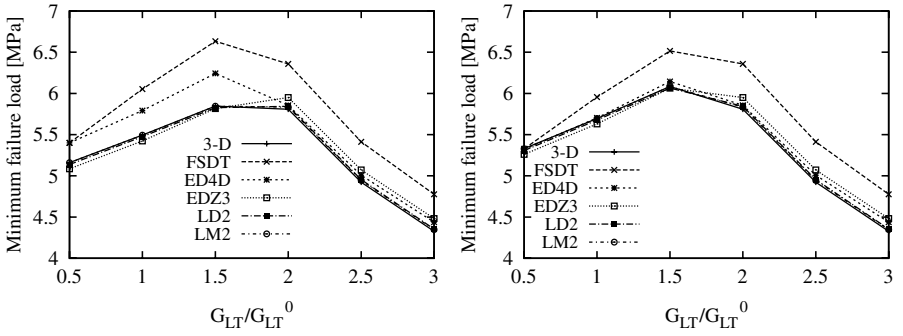


**Fig. 9 Minimum failure loads vs $G_{LT}/G_{LT}^0$ via the a) maximum stress and b) Hoffman criteria for $a/h = 10$.**

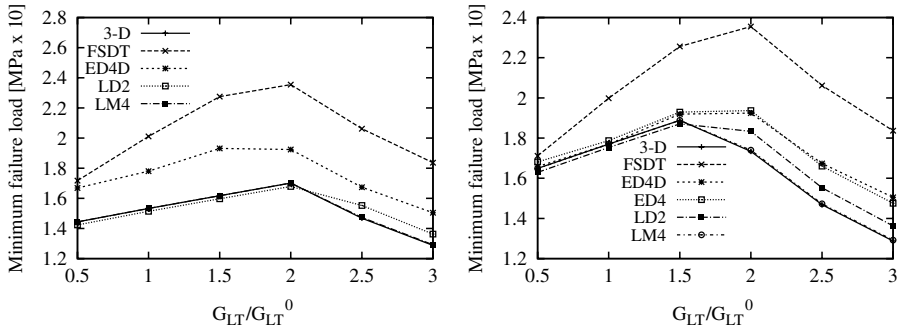


**Fig. 10 Minimum failure loads vs $G_{LT}/G_{LT}^0$ via the a) maximum stress and b) Hoffman criteria for $a/h = 5$.**

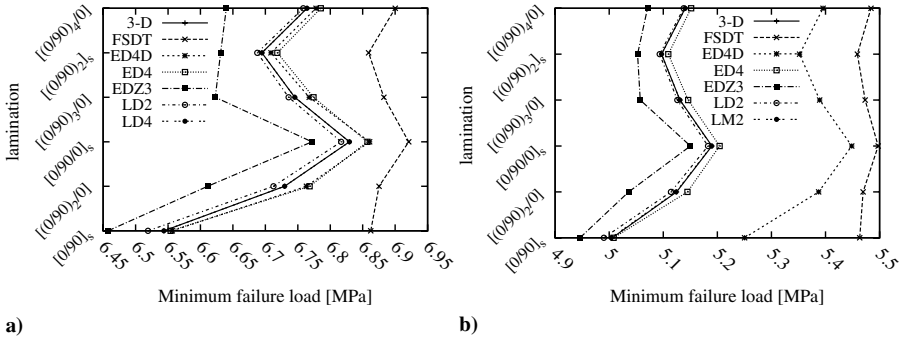


**Fig. 11 Minimum failure loads vs lamination sequence via the a) Tsai–Wu and b) Hashin criteria for $a/h = 10$.**

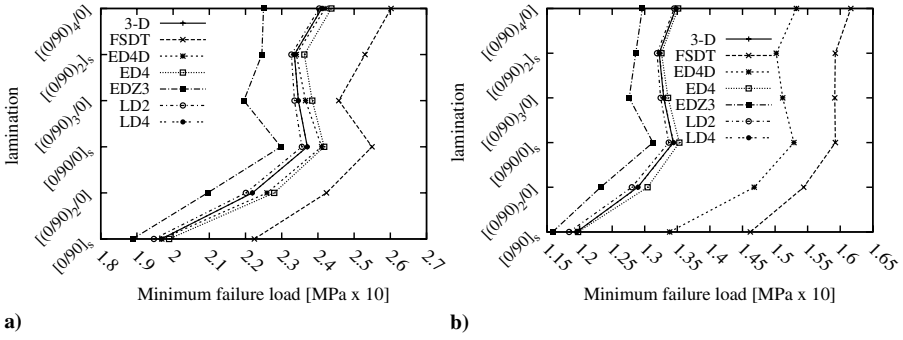


**Fig. 12 Minimum failure loads vs lamination sequence via the a) Tsai–Wu and b) Hashin criteria for $a/h = 5$.**

$a/h = 10$, the ED4 and EDZ3 models are accurate above the whole variation domain of $G_{LT}/G_{LT}^0$. This also holds for thick plates in the precritical part. The LW models match the exact solution.

### Influence of the Lamination Sequence

The influence of the lamination sequence is presented in Figs. 11 and 12. Relatively thick $a/h = 10$ and thick $a/h = 5$ plates are accounted for. The total laminate thickness is kept constant. 0 and 90 deg layers have been alternatively added in order to obtain a symmetrical stacking sequence. The results have been obtained via the Tsai–Wu and Hashin criteria. An analogous analysis can be found in Turvey [1,5] for angle-ply and antisymmetrically laminated cross-ply strips. The failure mechanics are not influenced by the stacking sequence, the failure locations being equal to those addressed in Tables 1–5. For $a/h = 10$, lamination $[0/90/0]_S$ yields

the maximum value of the failure loading. It is higher than the reference lamination layup by about 4%. In the case of thick plates, after a growth in correspondence to the first three configurations, the value remains almost constant. An improvement between 11% and 18%, with respect to the reference configuration, is obtained depending on the failure criterion. The considerations previously addressed about the two-dimensional models have been confirmed here.

#### Influence of the Loading Localization

The influence of the loading localization is investigated. The following localized loading is considered:

$$p_{zz}(x,y) = \begin{cases} p_{zz}^0 & \left(\frac{1}{2}-\frac{1}{k^*}\right) \le \left(\frac{x}{a},\frac{y}{b}\right) \le \left(\frac{1}{2}+\frac{1}{k^*}\right) 2 \le k^* \le 20 \\ 0 & \text{elsewhere} \end{cases} \tag{16}$$

The loading parameter $k^*$ ranges from 2 to 20. In the first case, loading covers the whole plate. In the last case, it is applied to an area equal to $a/10 \times b/10$. Increasing $k^*$, the failure loading increases because the loading application area is reduced. In terms of loading resultant, the more localized the loading, the more the failure resultant decreases. This is due to the fact that the ratio of the failure-loading resultant, for a generic value of $k^*$ and for the case of $k^* = 2$, is proportional to the ratio of the corresponding failure loadings by a term that is equal to $4/k^{*2}$. Increasing $k^*$, the decrement of the ratio $4/k^{*2}$ prevails on the growth of the failure-loading ratio. The variation in the minimum failure loading vs $k^*$ is presented in Figs. 13 and 14 for relatively thick and thick plates, respectively. For the sake of brevity, only the results obtained via the Tsai–Wu and Hoffman criteria are depicted. In the case of thin plates, FSDT yields accurate results, the error being about 1% for $k^* = 20$. For $a/h = 50$, the error is up to about 6%, in the case of maximum stress and Hashin criteria, and to 3% for the others. ED4D matches the exact solution in the case of the Tsai–Wu, Tsai–Hill, and Hoffman criteria, whereas the error is about 3% in the other two criteria. For $a/h = 20$, the error in the case of FSDT could be as high as 30%. In the case of the side-to-thickness ratio equal to 10, the error due to FSDT is bounded between 10% and 62%, it is halved for the ED4D model, and it is, at worst, about 5% for ED4. Quadratic LW models ensure an accuracy of 2%. Displacement-based and mixed fourth-order models yield highly accurate results for any value of $k^*$. This is also valid for thick plates.

## Conclusions

The determination of the minimum first-ply failure loading and the failure location for orthotropic plates has been treated. The maximum stress, Tsai–Wu, Tsai–Hill, Hoffman, and Hashin failure models have been adopted. The plates have been considered to undergo a uniform bending loading that acts on the top of the whole structure or on a localized area. The Navier-type closed-form solution has been assumed. Several two-dimensional theories have been accounted for. Such models have been formulated according to a unified and comprehensive formulation, known as Carrera's unified formulation (CUF). CUF is based on three main points: 1) the type of principle unknowns, displacements or displacements and normal, and shear transverse stresses, 2) the approximation level, equivalent single layer (ESL) or layerwise (LW), and 3) the through-the-thickness polynomial approximation order. CUF yields higher-order, two-dimensional theories that account for transverse shear as well as normal deformation, which ensure continuity of the out-of-plane stress components and model the through-the-thickness zig-zag behavior of displacements and out-of-plane stresses that are peculiar of laminate mechanics. Classical theories, based on the Kirchhoff–Love or Reissner–Mindlin kinematic hypotheses, represent particular cases. Pagano's three-dimensional exact solution has also been adopted. The accuracy of two-dimensional models has been verified via comparison with the exact solution. On this basis, a hierarchy has been established for the two-dimensional theories. The influence of the side-to-thickness ratio $a/h$ and the aspect ratio $b/a$ on the first-ply failure mechanics and on the two-dimensional theory accuracy has been investigated. Increasing $a/h$, the failure criteria yield different failure loadings. The difference is due to the manner in which each criterion accounts for the out-of-plane stress components. For $a/h \ge 50$, the considered two-dimensional models all yield accurate results. In the case of relatively thick plates $a/h = 10$, errors of about 5% and 10% affect the FSDT results. The

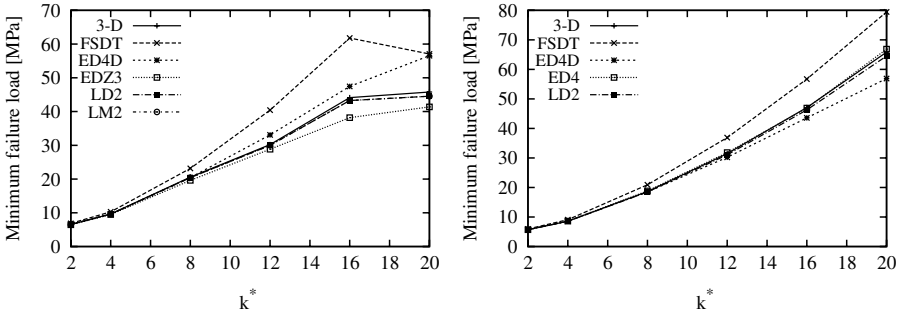


**Fig. 13 Minimum failure loads vs loading localization via the a) Tsai–Wu and b) Hoffman criteria for $a/h = 10$.**

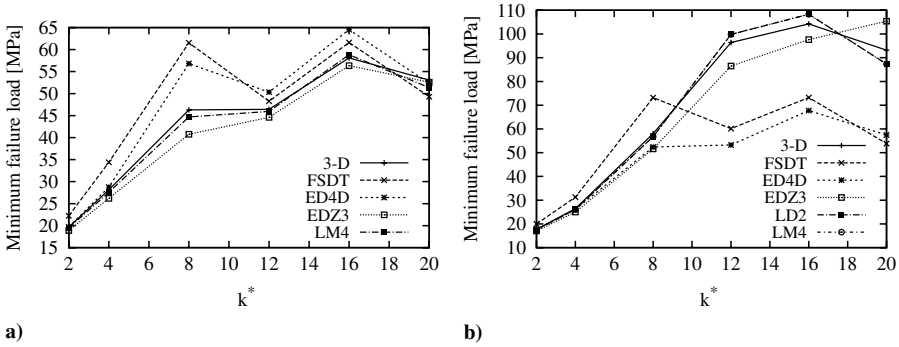


**Fig. 14 Minimum failure loads versus loading localization via the a) Tsai–Wu and b) Hoffman criteria for $a/h = 5$.**

maximum stress and Hashin criteria are the most sensitive to the two-dimensional model approximations. Fourth-order LW models match the exact solution, even in the case of very thick plates ($a/h = 2$). Increasing the aspect ratio, the failure criteria all predict the same failure loading and location. This is due to the fact that the mechanics of the plate degenerates into bending governed beam mechanics. The failure location shifts from the plate center to its corners. The dependency on the material properties $E_L/E_T$ and $G_{LT}$ has also been investigated. Increasing the degree of orthotropy, the accuracy of classical theories decreases. In the case of the maximum stress and Hashin criteria, the accuracy of higher-order models that discard the transverse deformation also decreases. Varying $G_{LT}$, a change in slope has been encountered. This is due to a change in the failure location/mechanics. Failure loading reaches a maximum in correspondence to a value of $G_{LT}$, which depends on the failure criterion. The accuracy of two-dimensional models has also been assessed by varying the stacking sequence and the loading application area. Higher-order models should be adopted in order to accurately predict failure mechanics in the case of localized loadings and $a/h \leq 10$.

## Acknowledgments

This research is supported by the Ministère de la Culture, de l'Enseignement Supérieuer et de la Recherche of Luxembourg under contract R&D BFR07/136-LB and two regional projects Piemonte 2004: E40 and E59.

## References

[1] Turvey, G. J., "A Study on the Onset of Flexural Failure in Cross-Ply Laminated Strips," *Fibre Science and Technology*, Vol. 13, No. 5, 1980, pp. 325–336. doi:10.1016/0015-0568(80)90008-1

[2] Turvey, G. J., "An Initial Flexural Failure Analysis of Symmetrically Laminated Cross-Ply Rectangular Plates," *International Journal of Solids and Structures*, Vol. 16, No. 5, 1980, pp. 451–463. doi:10.1016/0020-7683(80)90043-8

[3] Turvey, G. J., "Uniformly Loaded, Antisymmetric Cross-Ply Laminated, Rectangular Plates: An Initial Flexural Failure Analysis," *Fibre Science and Technology*, Vol. 16, No. 1, 1982, pp. 1–10. doi:10.1016/0015-0568(82)90010-0

[4] Turvey, G. J., "Initial Flexural Failure of Square, Simply Supported, Angle-Ply Plates," *Fibre Science and Technology*, Vol. 15, No. 1, 1981, pp. 47–63. doi:10.1016/0015-0568(81)90031-2

[5] Turvey, G. J., "Flexural Failure Analysis of Angle-Ply Laminates of GFRP and CFRP," *The Journal of Strain Analysis for Engineering Design*, Vol. 15, No. 1, 1980, pp. 43–49. doi:10.1243/03093247V151043

[6] Cauchy, A. L., "Sur l'Équilibre et le Mouvement d'une Plaque Solide," *Exercises de Matematique*, Vol. 3, 1828, pp. 328–355.

[7] Poisson, S. D., "Mémoire sur l'Équilibre et le Mouvement des Corps Élastique," *Mémoires de l'Académie des Sciences de Paris*, Vol. 8, 1829, pp. 357–570.

[8] Kirchhoff, G., "Über das Gleichgewicht und die Bewegung Einer Elastishen Sceibe," *Journal fur die Reine und Angewandte Mathematik*, Vol. 40, 1850, pp. 51–88.

[9] Turvey, G. J., "Effect of Shear Deformation on the Onset of Flexural Failure in Symmetric Cross-Ply Laminated Rectangular Plates," *Composite Structures*, Vol. 4, 1987, pp. 141–146.

[10] Reddy, J. N., "A Simple Higher Order Theory for Laminated Composites Plates," *Journal of Applied Mechanics*, Vol. 51, 1984, pp. 745–752.

[11] Liu, K. S., and Tsai, S. W., "A Progressive Quadratic Failure Criterion for a Laminate," *Composites Science and Technology*, Vol. 58, No. 7, 1998, pp. 1023–1032. doi:10.1016/S0266-3538(96)00141-8

[12] Kam, T. Y., and Jan, T. B., "First-Ply Failure Analysis of Laminated Composite Plates Based on the Layerwise Linear Displacement Theory," *Composite Structures*, Vol. 32, Nos. 1–4, 1995, pp. 583–591. doi:10.1016/0263-8223(95)00069-0

[13] Reddy, J. N., *Mechanics of Laminated Composite Plates and Shells. Theory and Analysis*, 1st ed., CRC Press, Boca Raton, FL, 1997.

[14] Tsai, S. W., and Wu, E. M., "A General Theory of Strength for Anisotropic Materials," *Journal of Composite Materials*, Vol. 5, No. 1, 1971, pp. 58–80. doi:10.1177/002199837100500106

[15] Hoffman, O., "The Brittle Strength of Orthotropic Materials," *Journal of Composite Materials*, Vol. 1, No. 2, 1967, p. 200. doi:10.1177/002199836700100210

[16] Kam, T. Y., Sher, H. F., Chao, T. N., and Chang, R. R., "Predictions of Deflection and First-Ply Failure Load of Thin Laminated Composites Plates via the Finite Element Approach," *International Journal of Solids and Structures*, Vol. 33, No. 3, 1996, pp. 375–398. doi:10.1016/0020-7683(95)00042-9

[17] Karmakar, A., and Sinha, P. K., "Impact Induced Dynamic Failure of Laminated Composite Pretwisted Rotating Plates," *Aircraft Engineering and Aerospace Technology*, Vol. 72, No. 2, 2000, pp. 142–155.

[18] Onkar, A. K., Yadav, D., and Upadhyay, C. S., "Probabilistic Failure of Laminated Composites Plates Using the Stochastic Finite Element Method," *Composite Structures*, Vol. 77, No. 1, 2007, pp. 79–91. doi:10.1016/j.compstruct.2005.06.006

[19] Reddy, J. N., and Pandey, A. K., "A First-Ply Failure Analysis of Composites Laminates," *Computers and Structures*, Vol. 25, No. 3, 1987, pp. 371–393. doi:10.1016/0045-7949(87)90130-1

[20] Pandey, A. K., and Reddy, J. N., "A Post First-Ply Failure Analysis of Composites Laminates," *Proceedings of the Twenty-Eighth International Conference on Structures and Structures Dynamics and Materials*, AIAA, New York, 1987, pp. 788–797.

[21] Reddy, Y. S. N., and Reddy, J. N., "Linear and Non Linear Failure Analysis of Composites Laminates with Transverse Shear," *Composites Science and Technology*, Vol. 44, No. 3, 1992, pp. 227–255. doi:10.1016/0266-3538(92)90015-U

[22] Reissner, E., "The Effect of Transverse Shear Deformation on the Bending of Elastic Plates," *Journal of Applied Mechanics*, Vol. 12, 1945, pp. 69–76.

[23] Mindlin, E., "Influence of the Rotatory Inertia and Shear in Flexural Motions of Isotropic Elastic Plates," *Journal of Applied Mechanics*, Vol. 18, 1951, pp. 1031–1036.

[24] Sih, G. C., and Skudra, A. M., *Failure Mechanics of Composites*, 1st ed., North-Holland, Amsterdam, 1985.

[25] Soni, S. R., "A New Look at Commonly Used Failure Theories in Composite Laminates," *Proceedings of the Twenty-Fourth International Conference on Structures and Structures Dynamics and Materials*, AIAA, New York, 1983, pp. 171–179.

[26] Soden, P. D., Hinton, M. J., and Kaddour, A. S., "A Comparison of the Predictive Capabilities of Current Failure Theories for Composite Laminates," *Composites Science and Technology*, Vol. 58, No. 7, 1998, pp. 1225–1254. doi:10.1016/S0266-3538(98)00077-3

[27] Hinton, M. J., and Soden, P. D., "Predicting Failure in Composite Laminates: The Background to the Exercise," *Composites Science and Technology*, Vol. 58, No. 7, 1998, pp. 1001–1010. doi:10.1016/S0266-3538(98)00074-8

[28] Puck, A., "A Failure Criterion Shows the Direction," *Kunststoffe*, Vol. 82, No. 7, 1992, pp. 29–32.

[29] Puck, A., and Schürmann, H., "Failure Analysis of FRP Laminates by Means of Physically Based Phenomenological Models," *Composites Science and Technology*, Vol. 58, No. 7, 1998, pp. 1045–1067. doi:10.1016/S0266-3538(96)00140-6

[30] Puck, A., and Schürmann, H., "Failure Analysis of FRP Laminates by means of Physically based Phenomenological Models," *Composites Science and Technology*, Vol. 62, Nos. 12–13, 2002, pp. 1633–1662. doi:10.1016/S0266-3538(01)00208-1

[31] Pinho, S. T., Dávila, C. G., Camanho, P. P., Iannucci, L., and Robinson, P., "Failure Models and Criteria for FRP Under In-Plane or Three-Dimensional Stress States Including Shear Non-Linearity," NASA TM-2005-213530, 1998, Feb. 2005.

[32] Basu, S., Waas, A. M., and Ambur, D. R., "Compressive Failure of Fiber Composites Under Multi-Axial Loading," *Journal of the Mechanics and Physics of Solids*, Vol. 54, No. 3, 2006, pp. 611–634. doi:10.1016/j.jmps.2005.09.004

[33] Basu, S., Waas, A. M., and Ambur, D. R., "A Macroscopic Numerical Model for Kink Banding Instabilities in Fiber Composites," *Journal of Mechanics of Materials and Structures*, Vol. 1, No. 6, 2006, pp. 979–1000.

[34] Basu, S., Waas, A. M., and Ambur, D. R., "Prediction of Progressive Failure in Multidirectional Composite Laminated Panels," *International Journal of Solids and Structures*, Vol. 44, No. 9, 2007, pp. 2648–2676. doi:10.1016/j.ijsolstr.2006.08.010

[35] Demasi, L., "$\infty^3$ Hierarchy Plate Theories for Thick and Thin

Composite Plates: The Generalized Unified Formulation," *Composite Structures*, Vol. 84, No. 3, 2008, pp. 256–270. doi:10.1016/j.compstruct.2007.08.004

[36] Reissner, E., "On a Certain Mixed Variational Theorem and a Proposed Application," *International Journal of Numerical Methods in Engineering*, Vol. 20, No. 7, 1984, pp. 1366–1368. doi:10.1002/nme.1620200714

[37] Carrera, E., "$C_z^0$ Requirements for the Two Dimensional Analysis of Multilayered Structures," *Composite Structures*, Vol. 37, Nos. 3-4, 1997, pp. 373–383. doi:10.1016/S0263-8223(98)80005-6

[38] Murakami, M., "Laminated Composites Plate Theory with Improved In-Plane Response," *Journal of Applied Mechanics*, Vol. 53, No. 3, 1986, pp. 661–666.

[39] Carrera, E., "Historical Review of Zig-Zag Theories for Multilayered Plates and Shells," *Applied Mechanics Reviews*, Vol. 56, No. 3, 2003, pp. 287–308. doi:10.1115/1.1557614

[40] Carrera, E., "On the Use of Murakami's Zig-Zag Function in the Modeling of Layered Plates and Shells," *Computers and Structures*, Vol. 82, No.7, 2004, pp. 541–554. doi:10.1016/j.compstruc.2004.02.006

[41] Carrera, E., "Theories and Finite Elements for Multilayered Plates and Shells: A Unified Compact Formulation with Numerical Assessment and Benchmarking," *Archives of Computational Methods in Engineering*, Vol. 10, No. 3, 2003, pp. 215–296. doi:10.1007/BF02736224

[42] Carrera, E., and Giunta, G., "Hierarchical Closed Form Solutions for Plates Bent by Localized Transverse Loadings," *Journal of Zhejiang University–Science A*, Vol. 8, 2007, pp. 1026–1037. doi:10.1631/jzus.2007.A1026

[43] Carrera, E., and Giunta, G., "Hierarchical Models for Failure Analysis of Plates Bent by Distributed and Localized Transverse Loadings," *Journal of Zhejiang University–Science A*, Vol. 9, No. 5, 2008, pp. 600–613. doi:10.1631/jzus.A072110

[44] Carrera, E., and Ciuffreda, A., "Bending of Composites and Sandwich Plates Subjected to Localized Lateral Loadings: A Comparison of Various Theories," *Composite Structures*, Vol. 68, No. 2, 2005, pp. 185–202. doi:10.1016/j.compstruct.2004.03.013

[45] Carrera, E., and Ciuffreda, A., "A Unified Formulation to Assess Theories of Multilayered Plates for Various Bending Problems," *Composite Structures*, Vol. 69, No. 3, 2005, pp. 271–293. doi:10.1016/j.compstruct.2004.07.003

[46] Carrera, E., and Demasi, L., "Two Benchmarks to Assess Two-Dimensional Theories of Sandwich, Composites Plates," *AIAA Journal*, Vol. 41, No. 7, 2003, pp. 1356–1362. doi:10.2514/2.2081

[47] Hashin, Z., "Failure Criteria for Unidirectional Fiber Composites," *Journal of Applied Mechanics*, Vol. 47, 1980, pp. 329–334.

[48] Pagano, N. J., "Exact Solutions for Rectangular Bidirectional Composites and Sandwich Plates," *Journal of Composite Materials*, Vol. 4, No. 1, 1970, pp. 20–34. doi:10.1177/002199837000400102

[49] Touratier, M., "An Efficient Standard Plate Theory," *International Journal of Engineering Science*, Vol. 29, No. 8, 1991, pp. 901–916. doi:10.1016/0020-7225(91)90165-Y

[50] Soldatos, K. P., "A Transverse Shear Deformation Theory for Homogeneous Monoclinic Plates," *Acta Mechanica*, Vol. 94, No. 3–4, 1992, pp. 195–220. doi:10.1007/BF01176650

[51] Carrera, E., "A Priori vs a Posteriori Evaluation of Transverse Stresses in Multilayered Orthotropic Plates," *Composite Structures*, Vol. 48, No. 4, 2000, pp. 245–260. doi:10.1016/S0263-8223(99)00112-9